Accepted Manuscript

Needle-less electrospinning employed for calcium and magnesium phosphate coatings on titanium substrates

M. Streckova, T. Sopcak, R. Stulajterova, M. Giretova, L. Medvecky, A. Kovalcikova, K. Balazsi

PII: S0257-8972(18)30189-0
DOI: doi:10.1016/j.surfcoat.2018.02.063
Reference: SCT 23134

To appear in: *Surface & Coatings Technology*

Received date: 13 December 2017
Revised date: 25 January 2018
Accepted date: 18 February 2018

Please cite this article as: M. Streckova, T. Sopcak, R. Stulajterova, M. Giretova, L. Medvecky, A. Kovalcikova, K. Balazsi , Needle-less electrospinning employed for calcium and magnesium phosphate coatings on titanium substrates. The address for the corresponding author was captured as affiliation for all authors. Please check if appropriate. Sct(2017), doi:10.1016/j.surfcoat.2018.02.063

This is a PDF file of an unedited manuscript that has been accepted for publication. As a service to our customers we are providing this early version of the manuscript. The manuscript will undergo copyediting, typesetting, and review of the resulting proof before it is published in its final form. Please note that during the production process errors may be discovered which could affect the content, and all legal disclaimers that apply to the journal pertain.

ACCEPTED MANUSCRIPT

Needle-less electrospinning employed for calcium and magnesium phosphate coatings on titanium substrates.

M. Streckova[a], T. Sopcak[a], R. Stulajterova[a], M. Giretova[a], L. Medvecky [a], A. Kovalcikova[a] K. Balazsi [b]

[a] *Institute of Materials Research, Slovak Academy of Sciences, Watsonova 47, 04 0 01 Kosice, Slovak Republic*

[b] *Institute of Technical Physics and Materials Sciences, Center for Energy Research, Hungarian Academy of Sciences, Konkoly Thege Miklós str. 29-33, 1121 Budapest, Hungary*

**Corresponding author: mstreckova@imr.saske.sk*

Phone number: +421-55-2342434

Fax: +421-55-6222124

Keywords: electrospinning; fibers; titanium substrate Ti6Al4V; coating; sol-gel method; in vitro tests

ACCEPTED MANUSCRIPT

ACCEPTED MANUSCRIPT

Abstract

The needle-less electrospinning method was employed for a preparation of calcium phosphate (CP) and magnesium calcium phosphate (MgCP) fibers as biocompatible coatings on Ti substrate. The polyvinylalcohol, triethyl phosphite, calcium and magnesium nitrates were used for a preparation of spun solutions and subsequent precursor fiber formation. The citric acid of 10 wt% was added to the spun solution in order to increase conductivity as well as a convenient complexing agent. A possible mechanism of complexation process of triethyl phosphite with calcium and magnesium nitrates with citric acid is presented. The optimization of calcination temperatures was defined according to the results obtained from TG/DSC analysis. The XRD analysis confirmed the formation of hydroxyapatite and Mg-whitlockite phases at both used temperatures 600 and 800 °C. The final morphology and thickness of prepared CP and MgCP fibrous coatings was designed by a suitable choice of the used sols, spinning time and calcination temperature. The SEM/FIB observations revealed that the average thickness of the CP coating was around 1 μm, which is almost two times thinner than the MgCP coating with the approximate width 2 μm. The in vitro cytotoxicity tests of the substrate surfaces revealed that the osteoblastic MC3T3-E1 cells have a good proliferation activity when cultured on the 600°C calcined substrates covered by smooth and uniform fibrous nets. A strong cytotoxic cell response was observed in the samples treated at 800°C, where the fibrous coatings were disrupted by the newly formed sharp rutile (TiO_2) micro-crystals. Such surface topography acts against the initial adhesion and proliferation of osteoblast like cells.

ACCEPTED MANUSCRIPT

1. Introduction

There are many metallic alloys, which are currently used as implant materials in clinical practice [1]. Among them titanium and its alloys hold a predominant place in orthopedic and dental applications because of their good biocompatibility, resistance to corrosion and mechanical strength [2]. In spite of these advantages the main drawback of titanium alloys relates to the motion at the implant – bone interface as a result of inadequate material osseointegration with the host tissue [3]. The solution to this problem lies in creating a coating on implant surface with biological active layer, which can significantly improve the fixation properties and prevent implant failure [4]. Calcium phosphate (CP) bioceramics as a basic mineral part of connective tissue has been extensively used in various field of biomedical applications thanks to good bioactivity, osseointegration and osteoconductive properties [5]. Despite of excellent biological properties, the CPs are known as materials with low mechanical strength and toughness, which allow their use only as filling materials or coatings. The CP-based coatings, mainly in the most stable - hydroxyapatite (HAP) form, were deposited onto the metallic surface in order to maintain the high mechanical strength of implants in combination with notable biological properties of CP layers. The recently used deposition techniques include, for example, thermal plasma spraying [6], radio-frequency magnetron sputtering [7], dip coating [8], electrophoretic deposition [9], etc. The main disadvantage of high temperature deposition methods (e.g. plasma spraying) lies in a degradation of HAP phase during the heat treatment as well as controlling the thickness of deposited layers [10]. Nowadays, low-temperature electrohydrodynamic techniques like for instance electrospinning and electrospraying have received much attention in many different industrial areas due to capability of developing fibers or particles at micron, submicron or nanoscale range [11]. The basic principle of electrospinning is based on generating free charges

ACCEPTED MANUSCRIPT

on the surface of polymer solution by a high voltage potential, which overcomes the solution's surface tension and produces a charged jet of conical shape usually gathered on grounded collector [12]. In a typical setting one or more needles (spinnerets) are generally used to drawn the fibers from solutions or melt. However, the production rate of the simple spinneret is very low, which implies strong limitations for mass production [13]. On the other hand, the needle-less (NLE) or free liquid surface electrospinning can generate numerous jets from the solution surface what enhances the production rate even one or two orders of magnitude in comparison with the conventional method [13,14].

Although the electrospinning is considered as a powerful fiber producing technique, only a few previous studies dealt with the use of this method for the deposition HAP fibers on Ti surfaces. Iafisco et al. [15] has coated Ti alloy by the nanostructured collagen-apatite fibers by combining electrospinning and biomimetic mineralization. Their results showed that the obtained mineralized scaffolds are quite similar to natural bone extracellular matrix from the morphological, structural, and compositional point of view. Santhosh and Balasivanandha Prabu [16] electrospun coated Ti-6Al-4V alloy with nano HAP – polysulfone. It was demonstrated that the coating containing nano HAP particles promoted growth of apatite crystals upon immersion in simulated body fluids (SBF) and did not show corrosion over prolonged soaking of 14 days.

Recently, growing interest has been devoted to a production of Mg containing biomaterials such as biocements [17], scaffolds [18] and coatings on metallic substrates [19-21] due to the beneficial biological effect of Mg emerging as a naturally occurring element in human body, especially in bones [22]. The Mg containing calcium phosphates (MgCP), such as Mg substituted hydroxyapatite (Mg-HAP), has been shown as an attractive component to improve the biocompatibility of HAP coatings. For instance, Zhao *et al*. [20] electrochemically deposited pure HAP and Mg-HAP coatings on the surface of pure titanium discs. They showed that the Mg-HAP

ACCEPTED MANUSCRIPT

coated surfaces promoted osteogenic differentiation of preosteoblasts *in vitro* and improved implant osseointegration during the early stages of bone healing as compared with the pure HAP coated surfaces. The CP biomimetic coatings doped with Mg^{2+}, Sr^{2+} and Mn^{2+} were also recently developed in order to improve the biological performance of Ti implants [21]. The results of the in-vitro test showed that the Mg and Sr doped apatite coatings exhibit a higher adhesion and proliferation of osteoblastic cells with respect to pure Ti or the thin layer of amorphous phosphate coating obtained in the presence of Mn.

The present work is focused on a design of the bioceramic CP and MgCP coatings via needle-less electrospinning method. The CP and MgCP coatings were prepared by the sol-gel method from solutions containing calcium/magnesium nitrates and triethyl phosphite with the Ca/P and Ca+Mg/P ratios set to 5:3. The citric acid was used as a complexing agent as well as for the necessary higher conductivity of the prepared sols. The complexation mechanism of precursor sols was suggested. The coatings were deposited on commercially Ti–6Al–4V discs and thermal treated at two different temperatures (600 or 800°C). The effect of used temperatures on morphology, density and thickness of fibrous samples was thoroughly described by SEM/FIB analysis. The in vitro osteoblast response of final deposited fibrous coatings was also investigated.

2. Materials and methods

2.1 Preparation of sols for electrospinning

The CP and MgCP precursors were prepared by the sol-gel method using triethyl phosphite (TEP), calcium nitrate tetrahydrate ($Ca(NO_3)_2 \cdot 4H_2O$) and magnesium nitrate hexahydrate ($Mg(NO_3)_2.6H_2O$) all purchased from Sigma-Aldrich, USA, respectively. TEP (10.4

ACCEPTED MANUSCRIPT

ml) was firstly diluted in 20 ml deionized water. The $Ca(NO_3)_2 \cdot 4H_2O$ (23.8g) was dissolved in 20 ml water and dropwise added into phosphate solution (Ca/P ratio = 5:3) under vigorous mixing (400 rpm, 2 h, RT). Following, 5 g of citric acid (CA) was admixed to the CP solution and the resulting mixture was aged at 80°C for 8 h. The MgCP precursor sol was produced similarly as CP sol, first by dissolving $Ca(NO_3)_2 \cdot 4H_2O$ (11.8 g) and $Mg(NO_3)_2.6H_2O$ (12.8 g) in 20 ml water and adding the mixed Ca + Mg solution to TEP (10.3 ml in 20 ml water) solution. The (Ca+Mg)/P ratio was also kept at the constant value 5:3. The final solutions for electrospinning were prepared by mixing 10 wt% of polyvinyl alcohol (PVA, Acros Organic, Mw = 85.000-124.000 $g.mol^{-1}$) water solution with the prepared sols at the ratio 2:1. The notation of the samples before and after calcination process is summarized in the Tab. 1.

2.2 Substrate preparation

All prepared coatings were spinned first on the basic textile substrate - polypropylene non woven spun-bond in order to optimize the conditions for NLE process. The final optimized sols were deposited on commercially pure Ti alloy (Ti6Al4V discs with diameter 35 mm, thickness 2 mm, sandblasted with 60 μm (180 grit) size corundum particles (Al_2O_3) purchased from PROTETIM Kft., Hungary). Before deposition, Ti substrates were ultrasonically cleaned in acetone for 20 min and air dried.

2.3 Electrospinning deposition of CP and MgCP coatings

The needle-less electrospinning device (NLE, Nanospider TM NS Lab from ELMARCO) was used for the deposition of CP and MgCP fibers on Ti substrate by the following procedure: the solutions for electrospinning were loaded into the spinning bath (30 ml vessel and rotating electrode) and the distance between spinning and collector electrodes was adjusted to 140 mm.

ACCEPTED MANUSCRIPT

The rotation speed of the spinning electrode was set to 10 rpm and subsequently a high voltage of 70 – 75 kV was exposed on the spinning drum surface. The four different times 3,5,10 and 20 min were used for optimization of the electrospinning process on Ti substrate at room temperature (RT) with a relative humidity of 60%. Electrospun fibrous mats were stabilized at 80°C/0.5 h and subsequently calcined at 600 and 800°C for 6 h at the heating rate of 10°C/min.

2.4 Characterization methods

The conductivity measurement of sols was performed on the HANA HI 9033 conductometer. The thermal decomposition of the samples was analyzed by differential scanning calorimetry supplemented with thermogravimetric analysis (DSC/TG, JUPITER STA 449-F1 NETZSCH) in air atmosphere with heating rate of 10°C/1min. The phase composition of samples were investigated by the X-ray diffraction analysis (XRD, PhilipsX' PertPro,CuKα radiation; 2θ in the range of 10 - 60 °, 40kV, 50mA). The surface morphology and microstructure of CP and MgCP precursors and final calcined fibers was studied by scanning electron microscopy (SEM/FIB, ZEISS AURIGA COMPACT). The microstructure of fibrous samples was observed after coating with a thin gold layer.

2.5 Cell viability test

The preosteoblastic MC3T3E1 cells (Sigma-Aldrich) were released from culture flasks after reaching confluence (SPLLife Sciences, Korea) enzymatically (0,25 % Trypsin-EDTA; Sigma). The cell population was counted (Neubauer hemacytometer) and adjusted to $4x10^4$ cells/1 ml of the culture EMEM (Eagles Mimumum Essential Medium, Sigma) medium with 10 % FBS (Fetal bovine serum, Biowest) and 1 % ATB-ATM (Antibiotic-antimycotic solution, Sigma-Aldrich). The specimens (7x7x2 mm sheets) were sterilized in the oven at 170 °C for 1

ACCEPTED MANUSCRIPT

hour and put in wells of the 48 well cell culture plate. The samples were pre-wetted with a complete culture medium for five minutes and the medium was removed. To each specimen in wells 500 µl of cell suspension with 2 x10^4 cells was added. Pure titanium sample with seeded cells was used as a positive control. The seeded cells were cultivated for selected times in an incubator (Memmert) at 37 °C, 5 % CO_2 and 95 % humidity with medium exchanged triplicate per week. After 48 hours and 10 days of cultivation, the cytotoxicity of coatings was examined with live/dead fluorescence staining and MTS proliferation test.

Fluorescein diacetate and propidium iodide were used for fluorescence staining. Fluorescein diacetate is reduced by viable cells to fluorescin and stains the viable cells green. Propidium iodide is permeable through damaged cell membranes of dead cells and stains the dead cells red. The fluorescence optical images were done by fluorescence optical microscope (Leica DM IL LED, blue filter).

The cell proliferation test was conducted by the commercially available Cell Titer Aqueus One Solution Cell Proliferation Assay (Promega, USA). The assay is based on the reduction of MTS tetrazolium compound by viable cells to a colored formazan product that is soluble in cell culture media. The formazan dye produced by viable cells was quantified by measuring the absorbance at 490 nm (Shimadzu UV1800).

3. Results and discussion

3.1 Conditions for preparation of spinned solution for NLE

Like any other technologies, NLE has also unique features, which must be necessarily fulfilled in order to produce the high-quality fibers. There are some specific processing parameters such as solution viscosity, conductivity, surface tension and solvent volatility which

ACCEPTED MANUSCRIPT

affect mainly the production of fibers through electrospinning. In general, the electrospinning process uses high voltage in order to overcome the surface tension of the solution droplets at the end of the needle or the surface tension of the liquid surface in NLE. Especially in the NLE, the ionic conductivity of solution plays a crucial role to generate sufficient number of charged particles which could be transferred to the solution surface. On the other hand, the highly conductive solution can cause extra charges which could not be accumulated on the liquid surface and hampered the generation of fibers from the fluid.

The sol for the preparation of spinned solution was taken according to Dai and Shivkumar [23]. However, the conditions and preparation of solution for spinning had to be adjusted due to the necessity of higher solution conductivity and stabilization of a precursor fibrous structure (Tab.1). As resulted from Tab. 1 it is clear, that despite of relatively high initial conductivity of the pure CP sol, its viscosity is to low for fiber production. The ionic conductivity of earlier published pure sol was 75 mS and further mixing of sol with PVA caused the decrease of solution conductivity as a result of an increase of the solution viscosity. Moreover, the prepared precursor fiber net was unstable and very sensitive to laboratory moisture immediately after the electrospinning process. Therefore we have added CA, a common tricarboxilic organic acid which in fact, similarly like other organic acids (acetic acid, trifluroacetic acid) [24]. decreased the solution surface tension and at the same time enhanced the charge density of PVA/solCP solution without significant effect on viscosity which resulted in easily spinable precursor fluid. The CA was added to the prepared CP and MgCP sols to achieve increase of conductivity and as a common complexing agent in aqueous-base sol-gel processes (see Scheme 1).The formation of calcium citrate complex led to a slight decrease of the sol conductivity, but the subsequent addition of PVA did not cause as significant decline of the conductivity as in the case of CA-free solution. The chosen ratio of both CP and MgCP sol to PVA was set up 1:2 and maintained for

ACCEPTED MANUSCRIPT

all prepared solutions. Moreover, CA can crosslinking with PVA through reaction of COOH groups of CA with the backbone chain of PVA.

Except of the conductivity, the effect of CA on the morphological structure of fibers is clearly evident from Fig.1a. The precursor fiber net spinned from sols without CA content did not show fibrous morphology due to the moisture instability (Fig. 1a). On the other hand, the resulted structure after calcination at 800 °C has shown porous but not fibrous structure of CP sample (Fig.1b). The precursor CP net prepared from the solution containing CA contrarily maintained the fibrous structure before as well as after the heat treatment (Fig.1c,d).

The comparison of thermal decomposition of pure PVA, PVA/solCP/CA and PVA/sol MgCP/CA precursor fibers was evaluated according to DSC/TG analysis (Fig.2a,b). It is obvious from Fig.2a that the overall weight mass loss of pure PVA can be separated into two temperature ranges. The evolution of weakly bonded water emerges in the first temperature range from 200°C to 250°C, while the decomposition of polymeric chain appears in the second temperature range from 250°C to 500°C. The first mass loss of PVA was invoked by the exothermic thermal process observed from DSC analysis (Fig.2b). The thermal degradation of PVA precursor fibers terminated at 500°C, above which no further mass loss was observed from TG analysis. In the case of PVA/solCP/CA and PVA/solMgCP/CA precursor fibers, the rapid decomposition and burning-out of citric calcium/magnesium-nitrate complexes (Scheme 1) was evident at 120°C indicated by the sharp exothermic peaks (see Fig.2b). A more gradual release and weight loss took place in the remaining temperature region, which is related with the degradation of PVA chain and formation of CP and MgCP phases. However, the continuous exothermic effect is evident in the temperature region from 300°C to 1000°C in the case of PVA/solCP/CA in contrast to PVA/solMgCP/CA precursor fibers. This effect is accompanied with the creation of

ACCEPTED MANUSCRIPT

CP phases. In addition, the sample transformation from the precursor PVA/solMgCP/CA was completed at lower temperatures than from the precursor PVA/solCP/CA.

Tab.1 Notation of the samples before and after the thermal treatment process. The composition of the solutions adjusted for spinning process according to ionic conductivity and applied voltage.

Precursor solutions	Sample	Ionic conductivity (mS)	Applied voltage (kV)	Final spinning
solCP	-	75	-	not spinable
solCP/CA	-	66	-	not spinable
PVA/solCP	-	58	75	slightly spinable
PVA/solCP/CA	CP	65	70	spinning
PVA/solMgCP/CA	MgCP	84	70	spinning

ACCEPTED MANUSCRIPT

ACCEPTED MANUSCRIPT

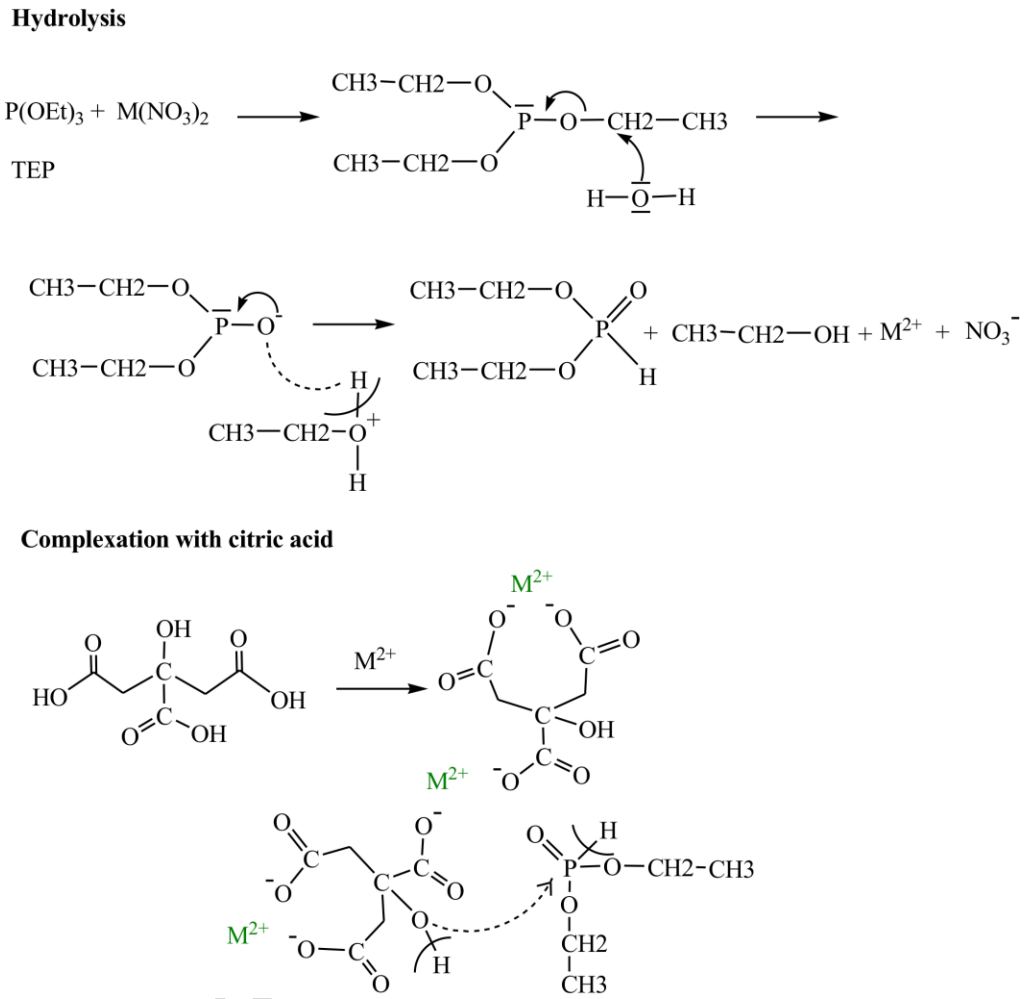

Scheme 1. The complexation process of triethyl phosphite with metal cations M^{2+} (calcium or magnesium) and citric acid.

ACCEPTED MANUSCRIPT

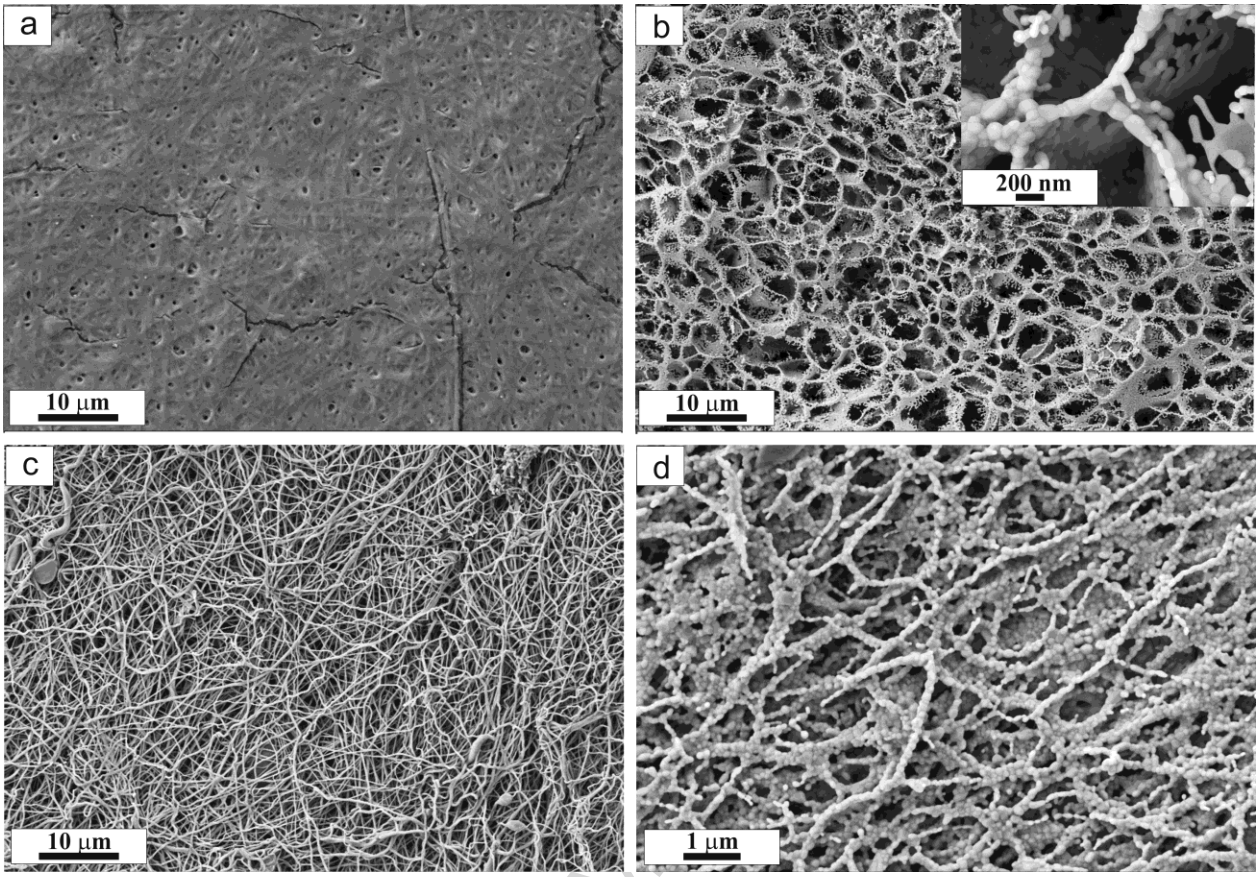

Fig.1 SEM image of electrospun fibers on textile substrate:
a) precursor fibers spinned from PVA/solCP,
b) calcined precursor fibers PVA/solCP at 800°C,
c) precursor fibers spinned from PVA/solCP/CA,
d) calcined precursor fibers PVA/solCP/CA at 800°C

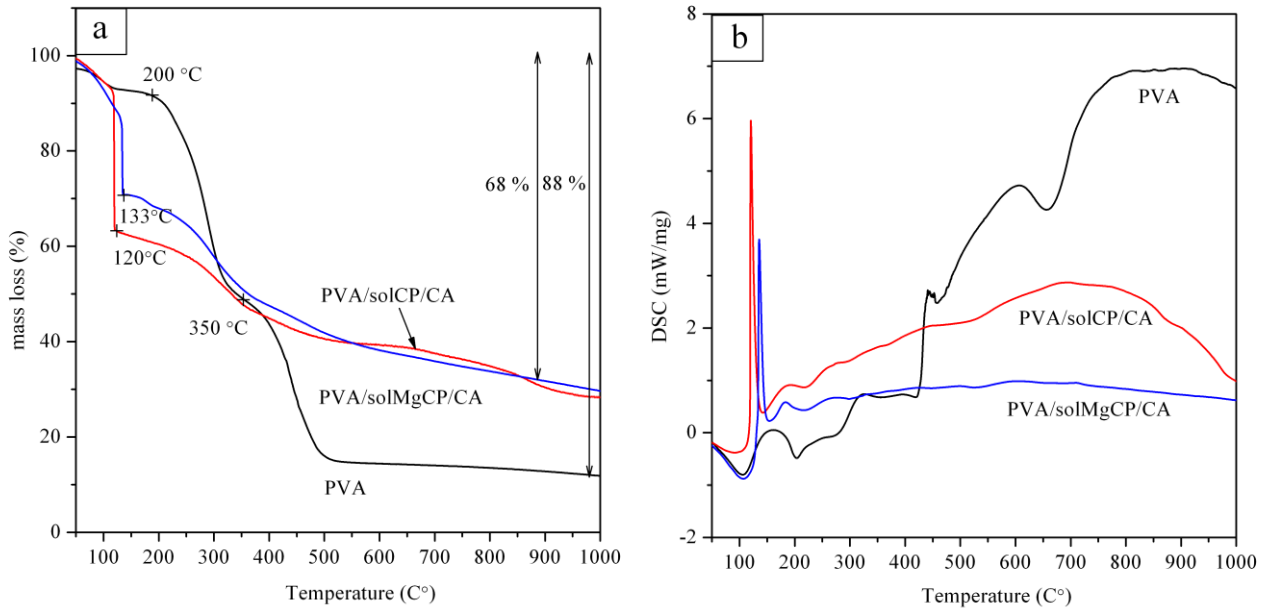

Fig.2 DSC analysis of fibers composed of pure PVA, PVA/solCP/CA, PVA/solMgCP/CA
a) TG analysis
b) DSC analysis

ACCEPTED MANUSCRIPT

3.2 XRD analysis

The XRD patterns of uncoated as received TiAl6V4 substrate to be further referred to as Ti substrate and the related substrates calcined one hour at 600°C or 800°C are shown in Fig.3a. The diffractogram of Ti substrate heat treated at 600°C shows only traces of rutile structure (TiO_2, JCPDS 01-1292) beside the main diffraction lines of the original Ti6Al4V phase. The rutile phase becomes more evident for Ti substrate calcinated at higher temperature 800 °C as a result of the pronounced oxidation of Ti.

Figs. 3b,c display the XRD patterns of the CP and MgCP fibers after the heat treatment at 600°C and 800°C, respectively. It can be observed from Fig.3b that both diffractograms indicate presence of the pure HAP phases (JCPDS 89-6440) with higher degree of crystallinity observed for the sample calcinated at 800 °C. On the other hand, the main diffraction pattern of MgCP fibers (Fig.3c) can be attributed to the Mg-whitlockite ($Ca_{18}Mg_2H_2(PO_4)_{14}$, JCPDS 70-2064) well crystallized at 800 °C with additional traces of the secondary MgO (JCPDS 89-7746) phase.

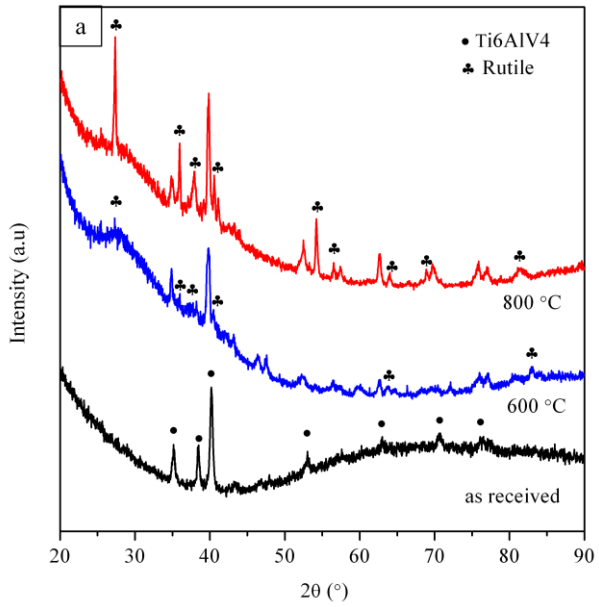

Fig.3a XRD pattern of as received and heat treated Ti6AlV4 substrates

ACCEPTED MANUSCRIPT

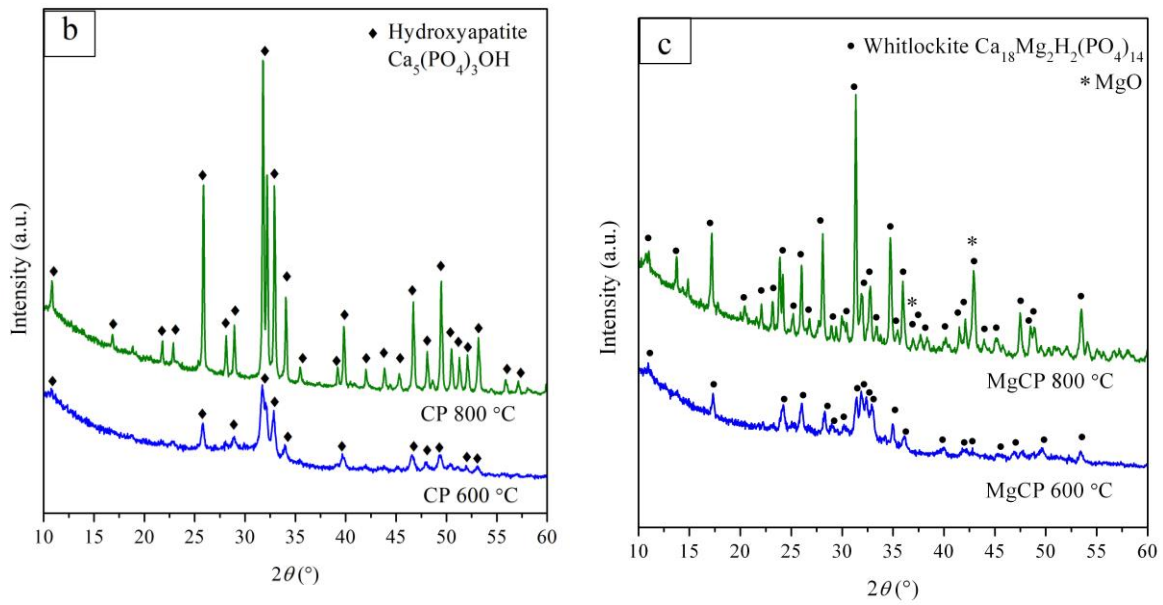

Fig. 3 XRD patterns of fibers calcined at 600 °C and 800 °C: b) CP and c) MgCP

3.3 Morphological characterization

The investigation of Ti6Al4V microstructure obtained after two different heat treatments is presented in Fig.4. The original microstructure of as received Ti6Al4V substrates is presented in Fig.4a,b in order to be capable of illustrating influence of the heat treatment. Surfaces of TiAl64V substrates were modified by sandblasting with Al_2O_3 microparticles, which were incorporated into the surface structure and were observed as large smooth microparticles with sharp edges (Fig.4b). The change in microstructure of Ti6Al4V surface affected by the lower calcination temperature 600°C is visible in Figs. 4c,d. The uniform spherical particles of rutile type resulting from the oxidation process can be clearly distinguished on the surface. The increase of the calcination temperature to 800 °C has caused the transformation of the rutile particles from a spherical to needle-like shape (Fig. 4e,f).

ACCEPTED MANUSCRIPT

Three different times of spinning process were compared in order to optimize the spinning time, density and consistency of prepared fibrous net: Fig.5a,b – 3min, Fig.5c,d – 5min, Fig.5e,f – 20 min. It is quite evident that the density of precursor fibrous net increases with increasing time of the spinning process (Fig. 5a,c,e). However, the spinning time of 20 minutes led to the formation of an excessively rough layer susceptible for exfoliation after calcination of samples at higher temperature (Fig. 5f). Besides the aforementioned features, the high surface shrinkage was also responsible for the exfoliation of prepared fibrous layer. Accordingly, 10 minutes for the spinning process has turned out to be optimal and was taken for all CP and MgCP fibrous coatings. The needle-like morphology of the rutile phase was obvious from all the calcined samples at 800 °C (Fig. 5b,d,f). It is tempting to conjecture that the needle-like morphology of the substrate prevents the formation of continuous fibrous net and promotes the exfoliation and disruption of the coating layer. Therefore, the calcination temperature 600 °C was taken for the final heat treatment of all prepared samples.

Fig. 6 compares SEM images for PVA/solCP/CA electrospun fibers obtained immediately after the spinning process in precursor form (Fig. 6a), after calcination of fibers at 600°C spinned on the textile substrate (Fig. 6b), after calcination of fibers at 800 °C spinned on the textile substrate (Fig. 6c) and CP fibers spinned for 10 minutes on Ti substrate and calcined at 600 °C (Fig. 6d). It follows from Fig. 7a that the precursor fibers were successfully prepared with quite uniform size in diameters without any droplets and defects. After calcination at 600°C, the CP particles were observed as interconnected spherical particles forming the linked chains (Fig. 6b). The calcination at 800°C led to a breakdown of fibrous structure, which is replaced with networks with highly interconnected porous scaffold (Fig. 6c). The similar observations were also found in the case of MgCP fibers prepared from PVA/solMgCP/CA on textile substrate (Fig. 7a,b,c). The fibrous morphology of the coatings was maintained after calcination temperature at

ACCEPTED MANUSCRIPT

600°C irrespective of the type of spinning substrates (textile or Ti substrate, see (Fig.7b,d). However, the higher density of fibrous mat was achieved in the case of MgCP coating compared with the pure CP coating on Ti substrate (Figs. 6d and 7d). Moreover, the Ti substrate clearly affected the morphology and density of CP and MgCP fibrous coating, since it was directly used as conductive substrate.

The focused ion beam technology (FIB) supplemented by the line EDX analysis was applied for verification of the coatings density and porosity after 10 minutes of spinning process (Figs. 8,9). The cross-section view on the CP and MgCP trenches milled by gallium ions is displayed in Figs. 8 and 9. It is quite evident that both fibrous coatings differ significantly in their morphology and final density. While the CP coating retained a clear fibrous morphology with a high amount of space between the individual fibers, the MgCP fibrous coating exhibited high density with a lower porosity. In addition, the average thickness of the CP coating was around 1 μm, which is almost two times thinner than the MgCP coating with the approximate width 2 μm (Figs. 8b,9b). The line EDX analysis provides the information about the chemical composition of prepared coatings in the direction marked with the yellow arrows (Figs. 8d, 9d). In both prepared coatings, the amount of Ca, Mg, P and O decreases in a spatial direction pointing into the deep of the trenches.

ACCEPTED MANUSCRIPT

ACCEPTED MANUSCRIPT

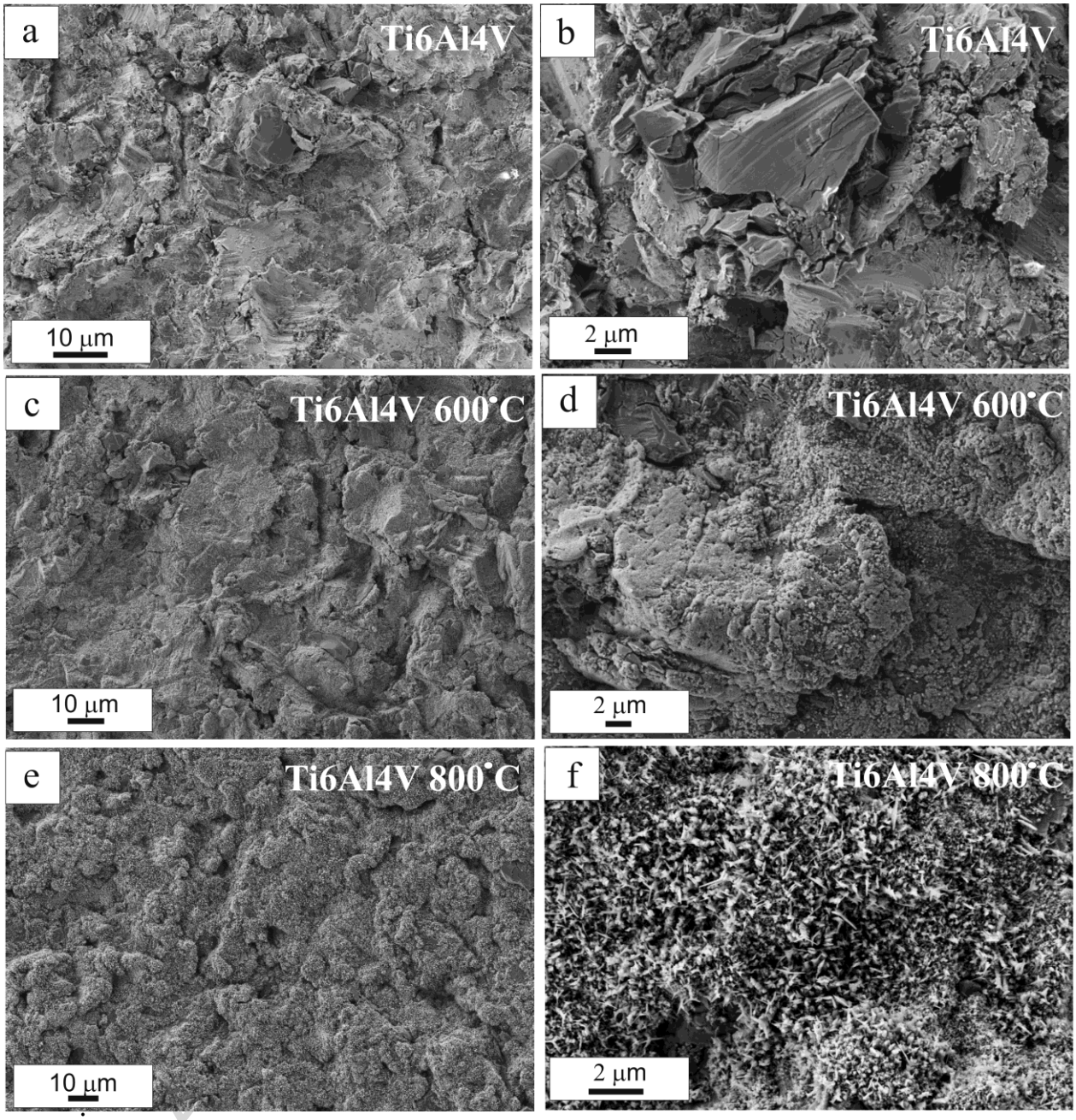

Fig.4 SEM images of Ti6Al4V affected by temperatures: a) as received, b) zoom of a, c) TiAl6V4 at 600°C, d) zoom of c, e) Ti6Al4V at 800°C, f) zoom of e.

ACCEPTED MANUSCRIPT

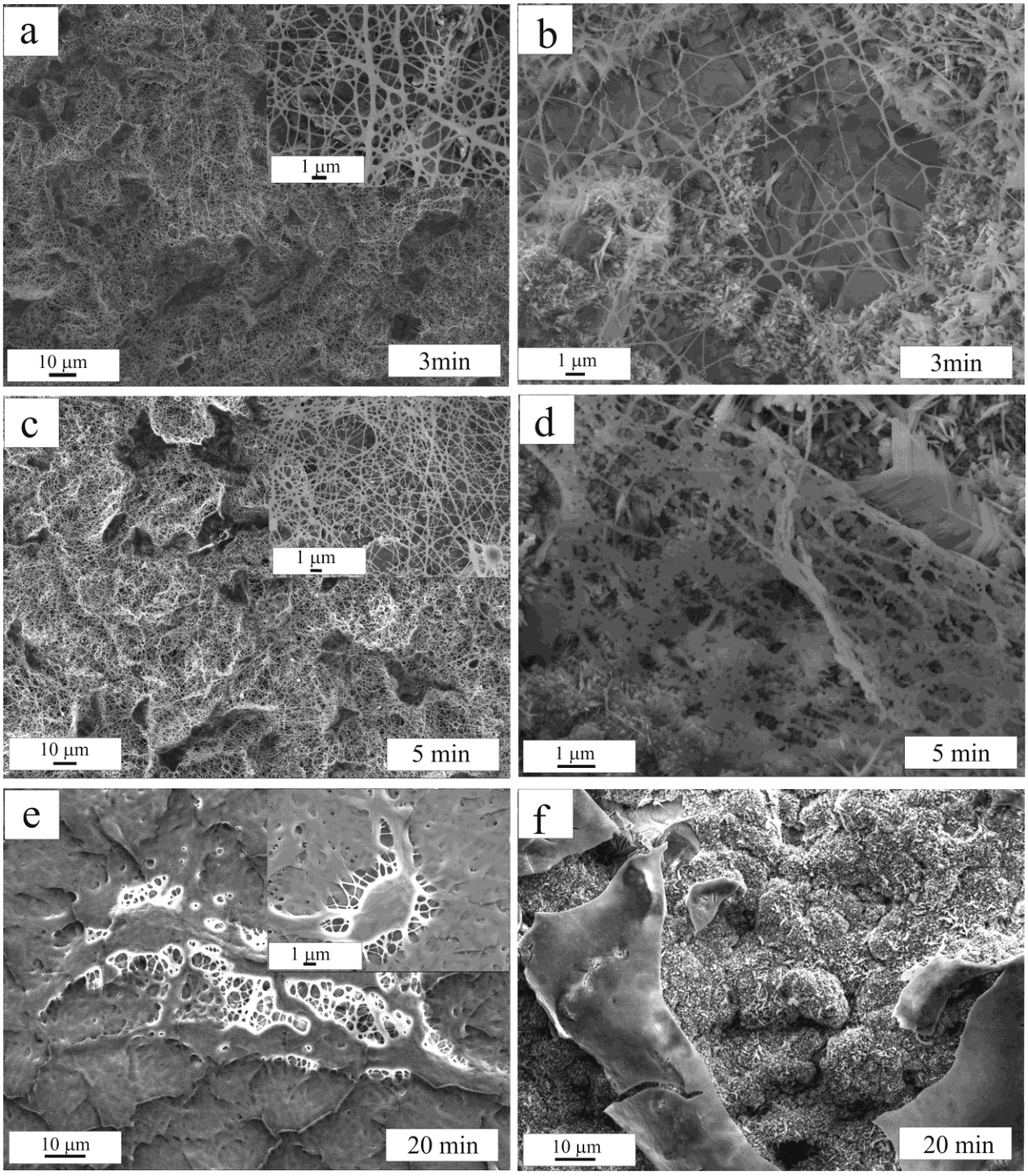

Fig.5 SEM images of CP coatings on Ti6Al4V substrate calcined at 800 °C and prepared at different times of spinning process: a) precursor fibers spinned for 3min. with zoom inside,
b) calcined sample spinned for 3 min.,
c) precursor fibers spinned for 5 min. with zoom inside,
d) calcined sample spinned for 5 min
e) precursor fibers spinned for 20 min. with zoom inside,
f) calcined sample spinned for 20 min

ACCEPTED MANUSCRIPT

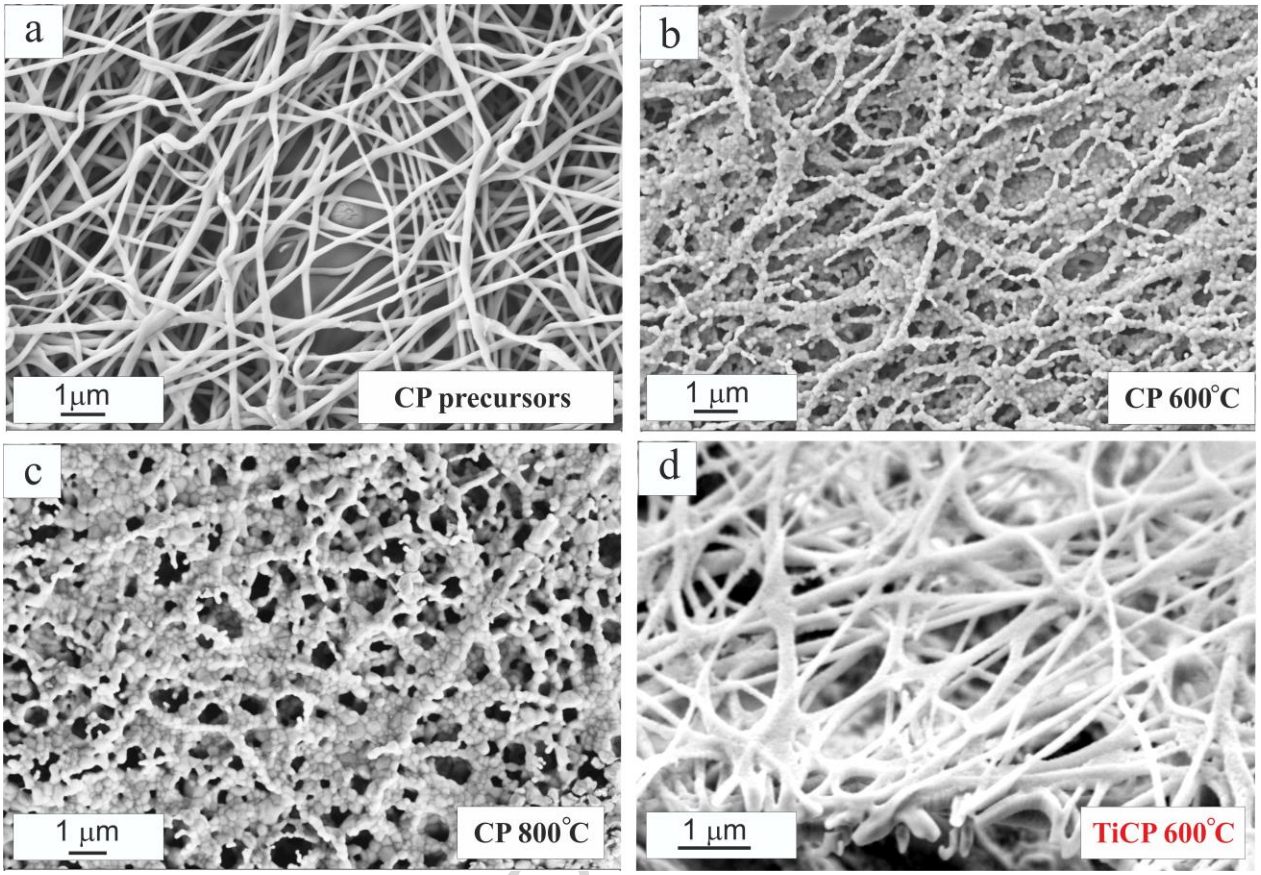

Fig.6 SEM images of CP coatings formed by: a) the precursor fibers spinned on the textile substrate, b) fibers calcined at 600 °C, c) fibers calcined at 800 °C, d) fibers calcined on Ti6Al4V substrate at 600 °C.

ACCEPTED

ACCEPTED MANUSCRIPT

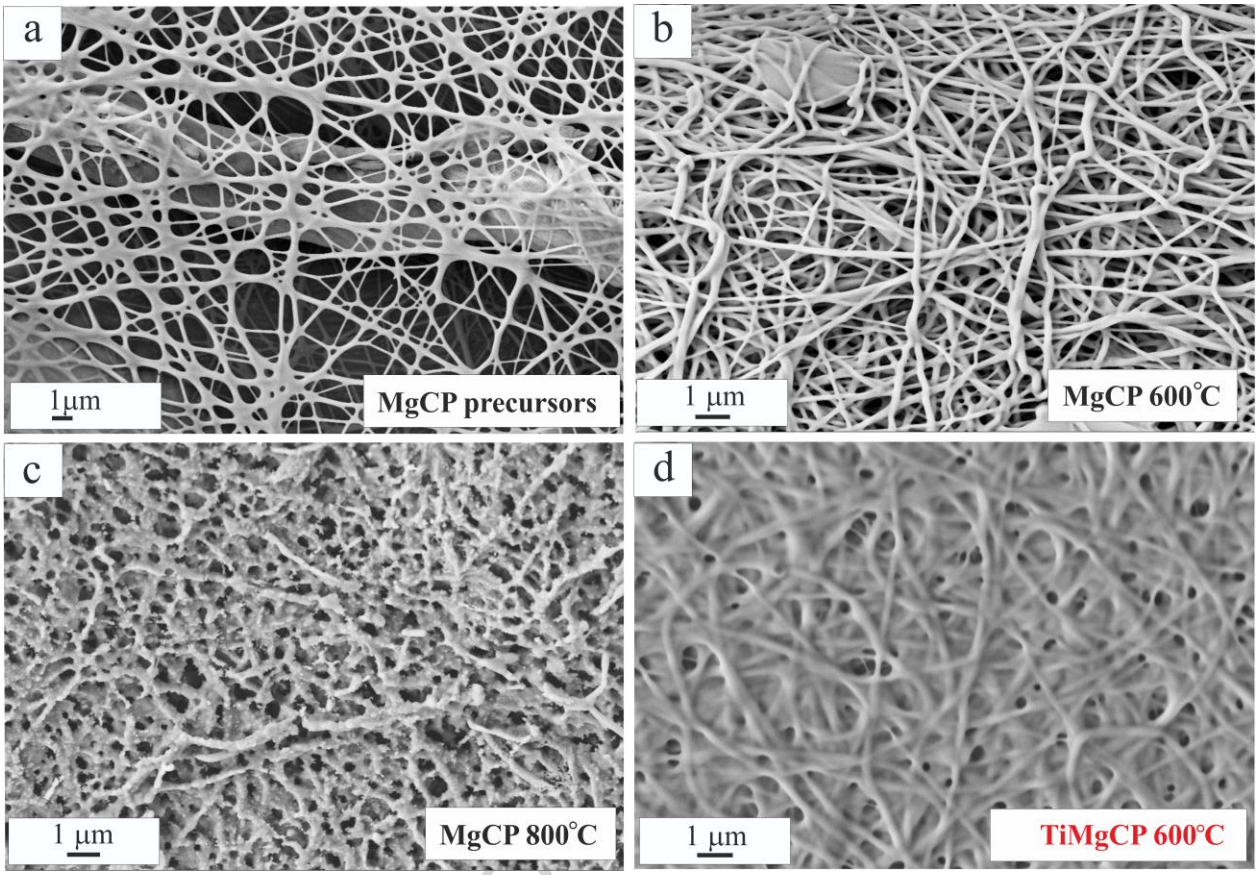

Fig.7 SEM images of MgCP coatings formed by: a) the precursor fibers spinned on the textile substrate, b) fibers calcined at 600 °C, c) fibers calcined at 800, °C d) fibers calcined on Ti substrate at 600 °C

ACCEPTED

ACCEPTED MANUSCRIPT

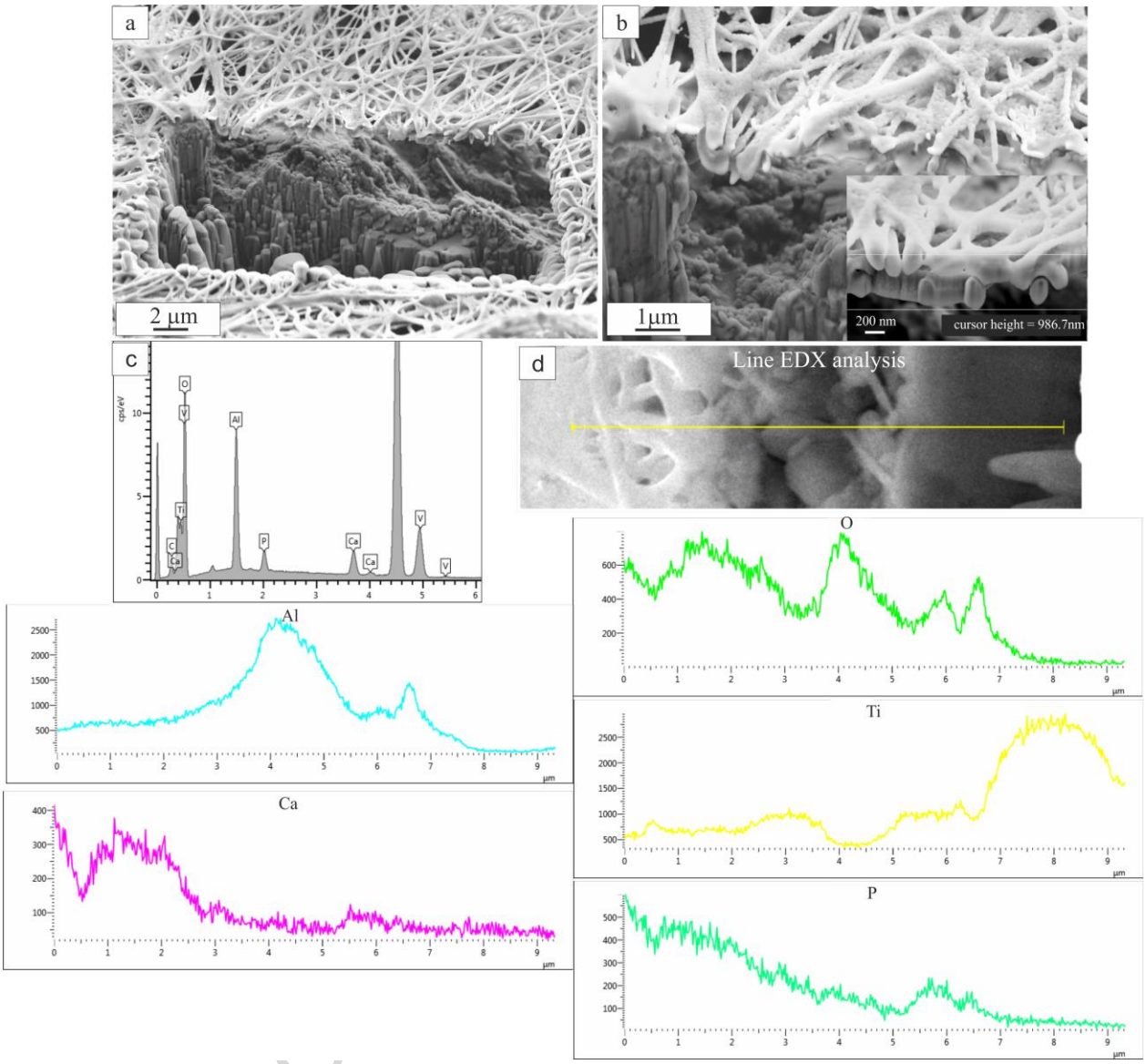

Fig.8

a) SEM/FIB image of the CP coating after 10 min. of spinning process and calcination at 600°C.
b) The detail on the CP coating with the direction of line analysis
c) EDX analysis with chemical composition of the CP fibrous coating.
d) The line EDX analysis in the direction depicted in Fig. 8b.

ACCEPTED MANUSCRIPT

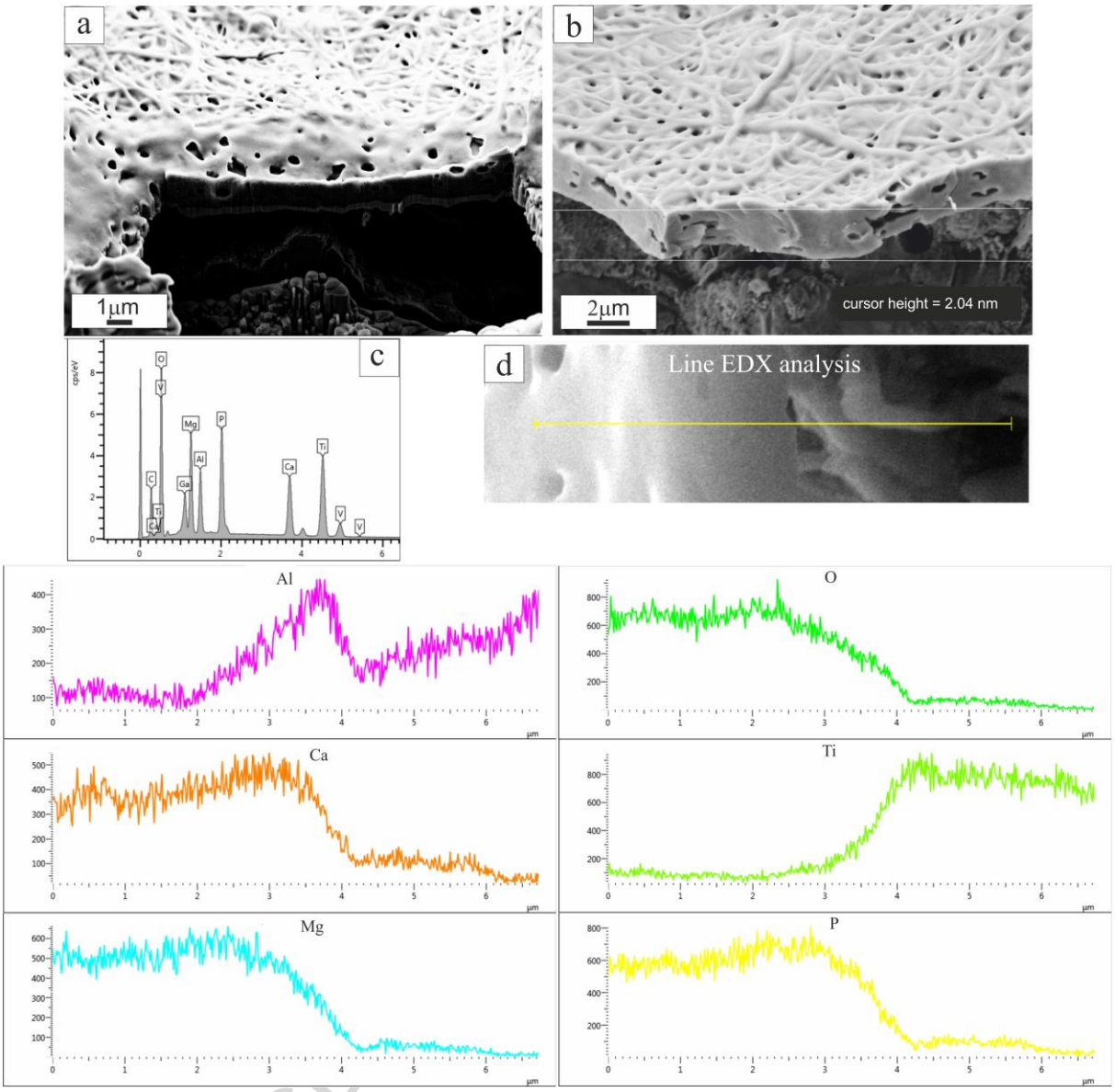

Fig.9
a) SEM/FIB image of the MgCP coating after 10 min. of spinning process and calcination at 600°C.
b) The detail on the MgCP coating with the direction of line analysis
c) EDX analysis with chemical composition of the CP fibrous coating.
d) The line EDX analysis in the direction depicted in Fig. 9b.

ACCEPTED MANUSCRIPT

3.4 Cell proliferation test

The evaluation of in vitro contact cytotoxicity testing (ISO 10993-5:2009; tests for in vitro cytotoxicity) of CP and MgCP coated titanium substrates annealed at 600°C and 800°C are shown in Fig.10. The relative proliferation of osteoblasts on samples are calculated as the ratio of formazan (absorbance of culture medium) produced by cells on calcined samples to formazan produced by cells on Ti6Al4V pure titanium sample. Fig.10 reveals a strong cytotoxicity of the CP and MgCP samples calcined at 800°C irregardless of the culture time. For the samples calcined at 600°C, the relative osteoblast proliferation on the surface of Ti samples coated with CP after 2 days cultivation and MgCP (both 2 and 10 days cultured) were not statistically different from 70% limit for cytotoxicity ($p>0.12$ and $p>0.81$ respectively). On the other hand, the CP after 10 days of culture was clearly noncytotoxic (statistically different from 70 % limit; $p<0.003$).

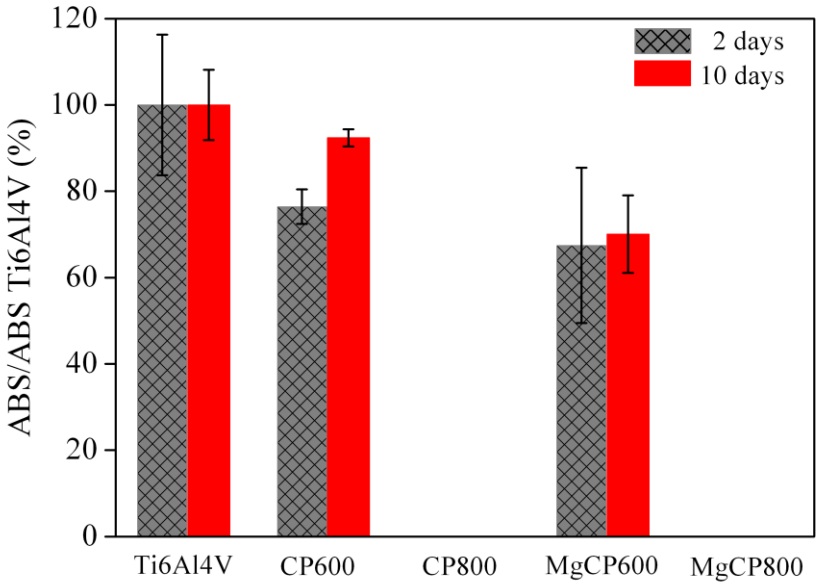

Fig. 10 Relative proliferation of cells on CP and MgCP coated Ti6Al4V surfaces after 2 and 10 days of cultivation in relation to cells proliferation on pure Ti6Al4V specimen with standard deviations.

ACCEPTED MANUSCRIPT

3.5 Live/dead fluorescence staining

The results from live/dead fluorescence staining are in accordance with the results obtained from the cell proliferation testing. The cells growing on pure titanium specimen (Fig. 11a) were well spread, adhered and uniformly distributed on surfaces after 2 days of cultivation. The cells have a prolonged morphology with filopodia mutually interconnected to each other cell. After 10 days of cultivation, the density of viable cells was significantly enhanced and cells created multilayer coating on surface (Fig. 12a). The prolonged cell morphology was clearly observed with visible filopodia without any dead cells.

After two days of cultivation, the Ti surfaces coated by 600°C calcined CP fibers showed viable cells with quite uniform distribution (Fig. 11b). Similar results were observed on the MgCP samples (Fig. 11d). However, the MgCP coated surface exhibited cells with longer filopodia, better spread on the sample in comparison with uncoated Ti. No dead cells were observed on sample surfaces. These facts clearly demonstrated that the cytotoxicity of CP and MgCP coated surfaces was low. After 10 days of cultivation (Fig. 12b,d) the strong population growth of osteoblasts was found on the surfaces, but some small regions without adhered cells can be also identified. A small difference in the density of live cells can be only found after 10 days of cultivation on CP surfaces where a denser cell layer was verified (Fig. 12b).

On the other hand, the strong cytotoxicity was revealed for both studied samples heat treated at 800°C irrespective of the cultivation time. Only a few live cells were identified on sample surfaces and the majority of cells were dead. Consequently, very small population of live poorly spread (spherical) and probably weakly adhered cells to surface of samples the 800°C calcined was observed after 10 days of culture (Figs. 11 and 12c,e).

ACCEPTED MANUSCRIPT

Such big differences in cells proliferation can be clearly attributed to the different surface microtexture of tested samples, which has already been proven in many cases of in vitro testing of biomaterials [25-27]. To confirm this fact, we have observed the microstructures and surface topographies of the CP and MgCP coated Ti substrates after 10 days of cultivation (Fig. 13). It can be seen from this figure that very fine needle-like rutile particles were formed on the whole substrate surfaces despite of using adequate spinning time, which was set to form continuous coating layers on the surface of Ti substrates in both CP and MgCP samples heat treated at 800°C. These newly formed sharp particles were perpendicularly oriented from the substrate surfaces and ruptured the fibrous nets. Consequently, the sharp edges of the rutile particles together with the exfoliated coatings did not allow good adherence of osteoblastic cells to the substrates and caused strong cytotoxicity. Some recent studies have been focused on studying the effect of Ti surface characteristics on the adhesion and proliferation of cells, which may be largely affected by the micro- and nanoscale topography, chemistry and charge distribution [28-30]. It has been demonstrated that different surface microstructures, e.g. globular, martensitic, bimodal and lamellar types, have been attained on the surface of Ti6Al4V alloy after using various surface treatments [31]. When applying the combination of the alkali - heat pretreatment techniques, a uniform porous sodium hydrogen titanate is formed on the origin substrate surface with the diffusion TiO_2 layer of thickness ranging from several hundreds of nm to several μm depending on the heat treatment temperature [32,33]. Su et al. [33] has pointed out that the presence of the sodium titanate layer was essential for preserving the surface and chemical composition of Ti6Al4V substrate after heat treatments performed at temperatures of 200 - 600°C as well as for ensuring the good adhesion and proliferation of osteoblasts. However, the heat treatment carried out at 800°C showed noticeable change in the surface morphology of substrate

ACCEPTED MANUSCRIPT

from the nanoporous network to a prismatic layer with crystals, which in turn resulted in the reappearance of toxic elements (Al and V) in the sodium titanate layer and hence decreased cell – surface attachment. According to Ref. [34], the heat treatment over 600°C of the alkali treated Ti causes a deterioration in the cohesion at the sodium titanate film–titanium interface due to the formation of rutile phase. In accordance with above studies we have also found that the upper limit for the heat treatment at 600°C. This temperature does not negatively affect the surface topography and the chemical composition of Ti substrate even if no chemical pretreatment is used. It has been found that the CP and MgCP coatings calcined at 600°C preserve their structural integrities, promote attachment and proliferation of osteoblastic cells. Therefore, the present study provides a new strategy of using the NLE technique for a production of coatings on Ti implants with possible applications in clinical practice. The exact mechanism how the fibrous nets were broken at elevated temperature of 800°C remains challenging task for future studies, which are of practical importance with regard to an elimination of the potential risks.

ACCEPTED MANUSCRIPT

ACCEPTED MANUSCRIPT

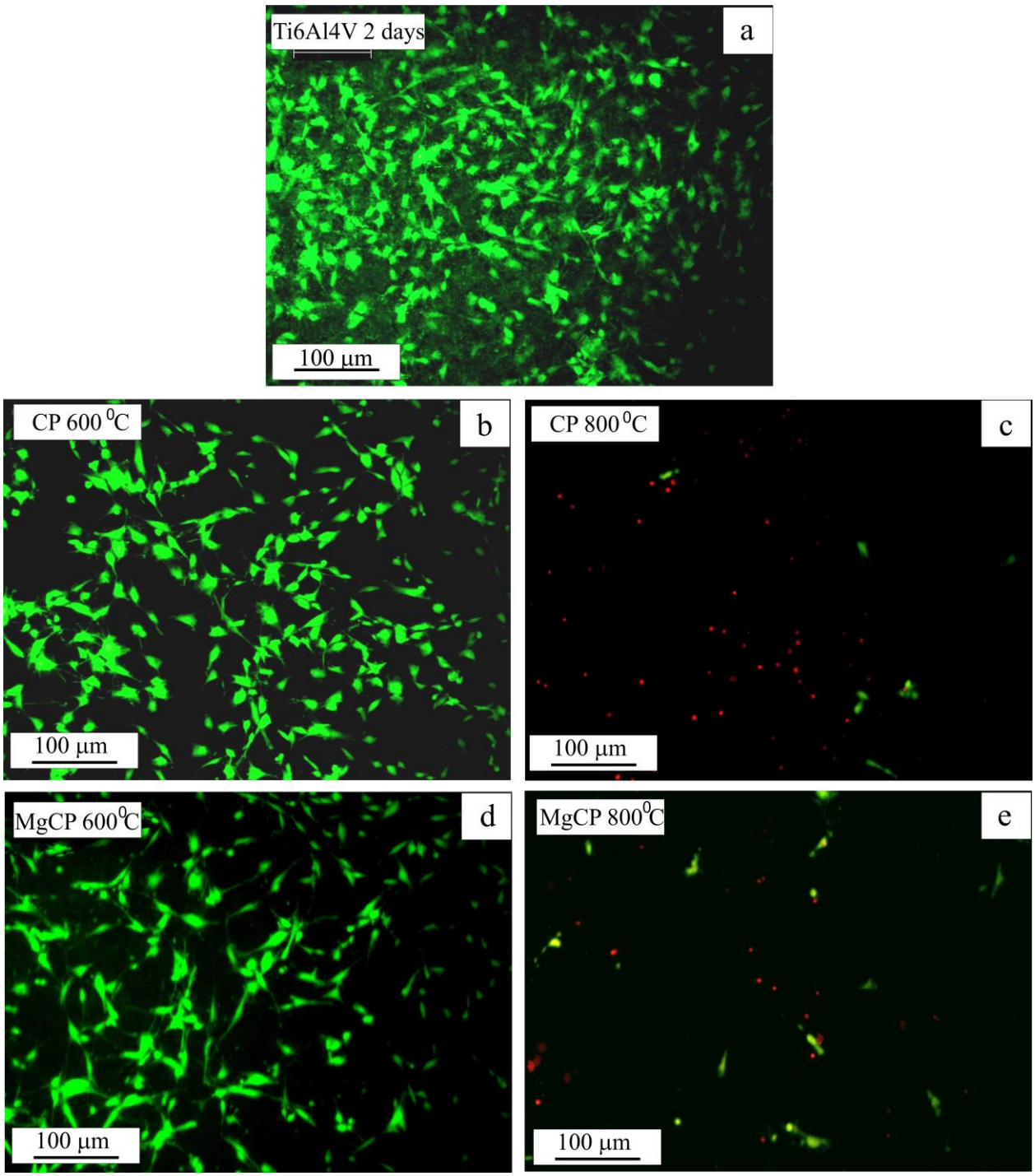

Fig.11 The morphology and density of osteoblastic cells on the Ti6Al4V surfaces after 2 days of cultivation. a) pure Ti6Al4V substrate
b) CP coated Ti6Al4V substrate calcined at 600°C
c) CP coated Ti6Al4V substrate calcined at 800°C
d) MgCP coated Ti6Al4V substrate calcined at 600°C
e) MgCP coated Ti6Al4V substrate calcined at 800°C

ACCEPTED MANUSCRIPT

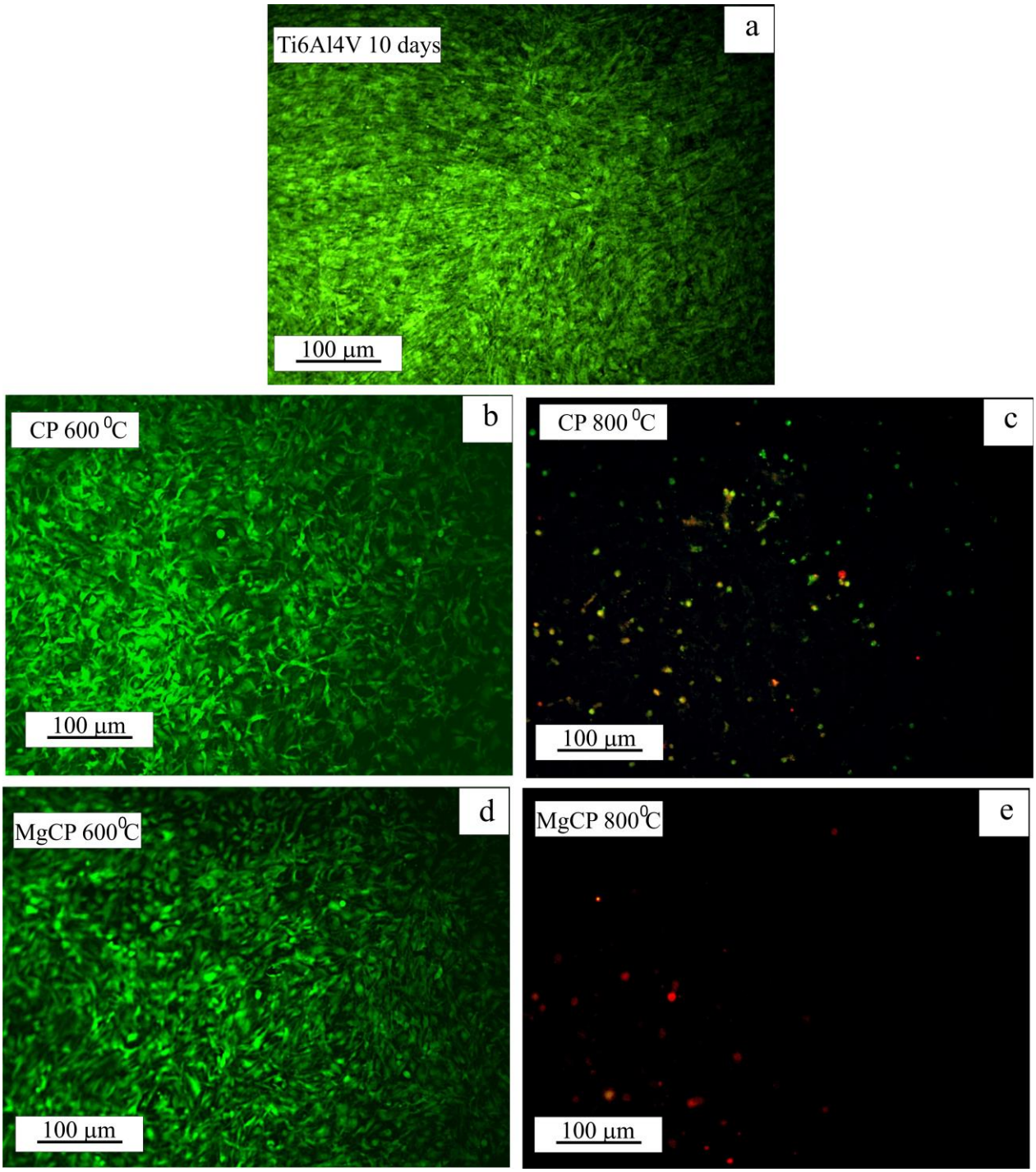

Fig.12 The morphology and density of osteoblastic cells on the Ti6Al4V surfaces after 10 days of cultivation. a) pure Ti6Al4V substrate
b) CP coated Ti6Al4V substrate calcined at 600°C
c) CP coated Ti6Al4V substrate calcined at 800°C
d) MgCP coated Ti6Al4V substrate calcined at 600°C
e) MgCP coated Ti6Al4V substrate calcined at 800°C

ACCEPTED MANUSCRIPT

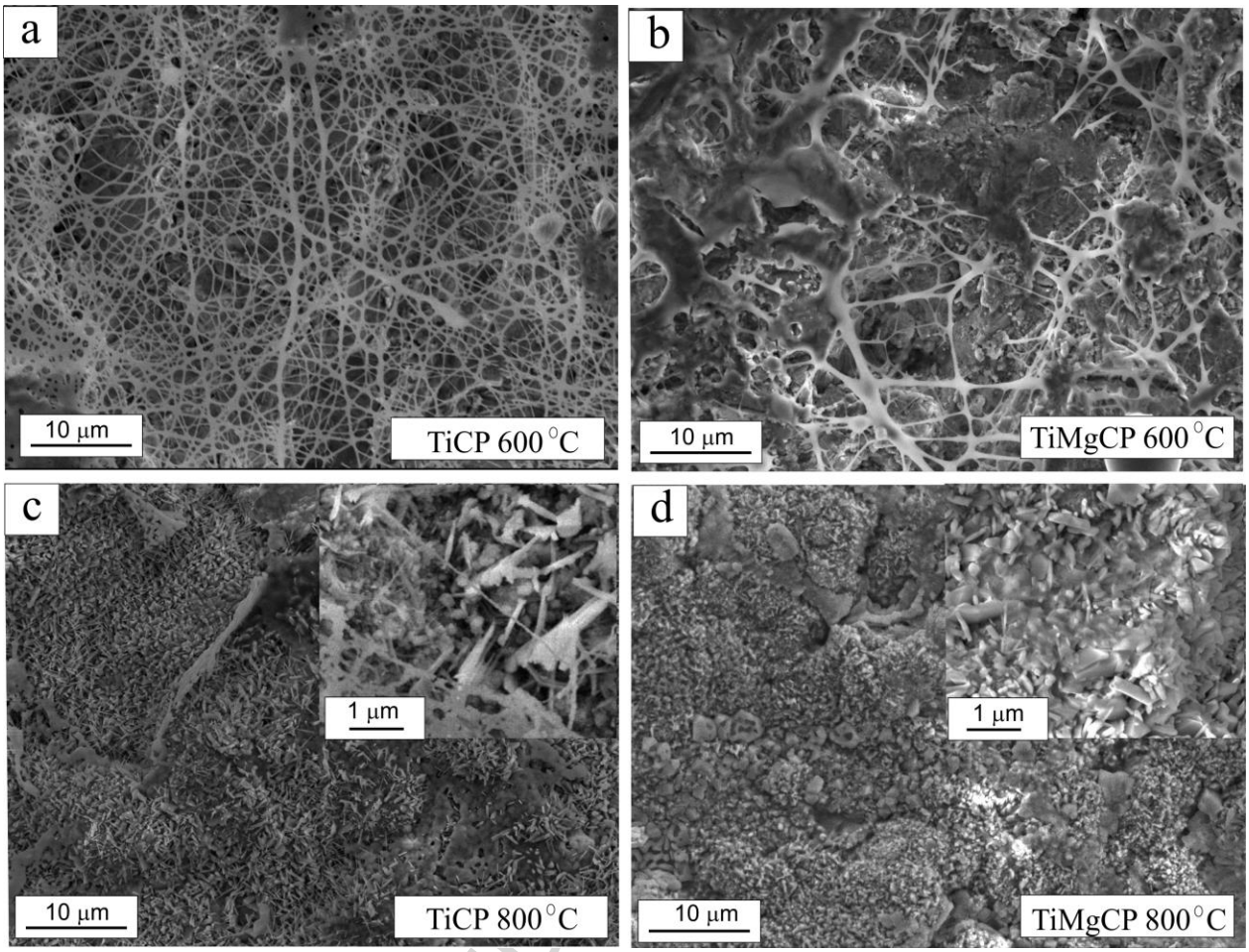

Fig. 13 Microstructure and surface texture of CP and MgCP coated Ti6Al4V substrates after 10 days of cell cultivation.

ACCEPTED

ACCEPTED MANUSCRIPT

4. Conclusion

The CP and MgCP fibers were successfully deposited on Ti substrate as a perspective biocompatible coating by means the simple needle-less electrospinning method. The proposed methodology for a preparation of such fibrous coatings essentially lies in its simplicity, low cost, and saving of time. The high performance of PVA-based CP and MgCP fibrous coatings can be achieved by optimization of conditions for: i) composition of sols, ii) addition of suitable complexing agent such as the citric acid and iii) careful thermal treatment preventing the substrate degradation. Several conclusions can be reached from a mutual combination of TG/DSC, XRD and SEM analyses. The XRD analysis demonstrated the transformation of precursor PVA/solCP/CA and PVA/solMgCP/CA to hydroxyapatite and Mg-whitlockite phases after both used heat treatment temperatures 600°C and 800°C. In agreement with our expectations, the higher crystallinity of both coatings was found in the samples calcinated at 800°C. However, it was discovered that the calcination of Ti substrates has significantly changed the morphology of growing rutile microparticles from a spherical to needle-like morphology. Simultaneously, in vitro cytotoxicity experiments showed that the coatings calcined at 600°C possess an excellent biocompatibility, spreading and proliferation of osteoblastic cells. On the other hand, the sample surfaces with a morphology strongly affected by higher calcination temperature 800°C revealed stronger cytotoxic character.

ACCEPTED MANUSCRIPT

Acknowledgement

This work was supported by the Scientific Grant Agency of the Ministry of Education, Science, Research and Sport of the Slovak Republic and the Slovak Academy of Sciences, projects No. VEGA 2/0079/17, 2/0047/17 and Slovak Research and Development Agency under the contract no. APVV 15-0115.

References

[1] I. Gotman, Characteristics of metals used in implants, J. Endourol. 11(6) (1997) 383-389.

[2] X. Liu, S. Chen, J.K.H. Tsoi, J.P. Matinlinna, Binary titanium alloys as dental implant materials — a review, Regen. Biomater. 4(5) (2017) 315–323.

[3] F. Javed, H. B. Ahmed, R. Crespi, G. E. Romanos, Role of primary stability for successful osseointegration of dental implants: Factors of influence and evaluation, Interv. Med. Appl. Sci. 5(4) (2013) 162 - 167.

[4] B.G. Zhang, D.E. Myers, G.G. Wallace, M. Brandt, P.F, Choong, bioactive coatings for orthopaedic implants - recent trends in development of implant coatings, Int. J. Mol. Sci. 15(7) (2014) 11878–11921.

[5] N. Eliaz, N. Metoki, Calcium phosphate bioceramics: A review of their history, structure, properties, coating technologies and biomedical applications, Materials (Basel). 10(4) (2017) 1-104.

[6] Y.C. Tsui, C. Doyle, T.W. Clyne, Plasma sprayed hydroxyapatite coatings on titanium substrates. Part 1: Mechanical properties and residual stress levels, 19(22) (1998) 2015-2029.

ACCEPTED MANUSCRIPT

[7] K. Ueda, T. Narushima, T. Goto, T. Katsube, H. Nakagawa, H. Kawamura, M. Taira, Evaluation of calcium phosphate coating films on titanium fabricated using RF magnetron sputtering, Mater. Trans. 48(3) (2007) 307-312.

[8] T. Li, J. Lee, T. Kobayashi, H. Aoki, Hydroxyapatite coating by dipping method, and bone bonding strength, J. Mater. Sci. Mater. Med. 7(6) (1996) 355-357.

[9] A.A. Abdeltawab, M.A. Shoeib, S.G. Mohamed, Electrophoretic deposition of hydroxyapatite coatings on titanium from dimethylformamide suspensions, Surf. Coat. Technol. 206 (2011) 43–50.

[10] R.B. Heimann, Editorial: Materials science of bioceramic coatings: An editorial, Open Biomed. Eng. J. 9 (2015) 25-28.

[11] J. A. Bhushani, C. Anandharamakrishnan, Electrospinning and electrospraying techniques: Potential food based applications, Trends Food Sci. Technol. 38(1) (2014) 21-33.

[12] K. Garg and G.L. Bowlin, Electrospinning jets and nanofibrous structures, Biomicrofluidics 5(1) (2011) 1-19.

[13] W.J. Liu, H.F. Zhang, D.W. Li, C. Huang, X.Y. Jin, Study on needle and needleless electrospinning for nanofibers, Adv. Mat. Res. 750-752 (2013) 276-279.

[14] O. Jirsak, S. Petrik, Recent advances in nanofibre technology: needleless electrospinning, Int. J. Nanotechnol. 9 (2012) 836–845.

[15] M. Iafisco, I. Foltran, S. Sabbatini, G. Tosi, N. Roveri, Electrospun nanostructured fibers of collagen-biomimetic apatite on titanium alloy, Bioinorg. Chem. Appl. 2012 (2012) 1-8.

[16] S. Santhosh, S. B. Prabu, Nano hydroxyapatite – polysulfone coating on Ti-6Al-4V substrate by electrospinning, Int. J. Mater. Res. 104(12) (2013) 1254 – 1262.

ACCEPTED MANUSCRIPT

[17] J. Jia, H. Zhou, J. Wei, X. Jiang, H. Hua, F. Chen, S. Wei, J.W. Shin, C. Liu, Development of magnesium calcium phosphate biocement for bone regeneration, J. R. Soc. Interface. 7(49) (2010) 1171–1180.

[18] J. Wei, J. Jia, F. Wu, S. Wei, H. Zhou, H. Zhang, J.W. Shin, C. Liu. Hierarchically microporous/macroporous scaffold of magnesium – calcium phosphate for bone tissue regeneration, Biomaterials 31 (2010) 1260–1269.

[19] J.F. Sun, Y. Han, K. Cui, Innovative fabrication of porous titanium coating on titanium by cold spraying and vacuum sintering, Mater. Lett. 62(21–22) (2008) 3623–3625.

[20] S.F. Zhao, Q.H. Jiang, S. Peel, X.X. Wang, F.M. He, Effects of magnesium-substituted nanohydroxyapatite coating on implant osseointegration, Clin. Oral Implants Res. 0 (2011), 1-8.

[21] B. Bracci, P. Torricelli, S. Panzavolta, E. Boanini, R. Giardino, A. Bigi, Effect of Mg^{2+}, Sr^{2+}, and Mn^{2+} on the chemico-physical and in vitro biological properties of calcium phosphate biomimetic coatings, J. Inorg. Biochem., 103 (2009) 1666-1674.

[22] S. Castiglioni, A. Cazzaniga, W. Albisetti, J.A.M. Maier, Magnesium and Osteoporosis: Current state of knowledge and future research directions, Nutrients. 5(8) (2013) 3022–3033.

[23] X. Dai, S. Shivkumar, Electrospinning of hydroxyapatite fibrous mats, Mater. Lett. 61 (2007) 2735–2738.

[24] O.V. Mukbaniani, M.J.M. Abadie, T. Tatrishvili, High-Performance Polymers for Engineering-Based Composites, first ed., Apple Academic Press, Oakville, 2015, pp. 327.

[25] S. Okada, H. Ito, A. Nagai, J. Komotori, H. Imai, Adhesion of osteoblast-like cells on nanostructured hydroxyapatite, Acta Biomater. 6 (2010) 591–597.

[26] E.A. dos Santos, M. Farina, G.A. Soares, K. Anselme, Chemical and topographical influence of hydroxyapatite and β-tricalcium phosphate surfaces on human osteoblastic cell behavior, J. Biomed. Mater. Res. 89 (2009) 510–520.

ACCEPTED MANUSCRIPT

[27] T. Sopcak, L. Medvecky, M. Giretova, A. Kovalcikova, R. Stulajterova, J. Durisin, Phase transformations, microstructure formation and in vitro osteoblast response in calcium silicate/brushite cement composites, Biomed. Mater. 11(4) (2016) art. no. 045013.

[28] T.K Monsees, K. Barth, S. Tippelt, K. Heidel, A. Gorbunov, W. Pompe, R.H.W. Funk, Effects of different titanium alloys and nanosize surface patterning on adhesion, differentiation, and orientation of osteoblast-like cells, Cells Tissues Organs. 180 (2005) 81–95.

[29] N. Ohtsu, T. Kozuka, M. Hirano, H. Arai, Electrolyte effects on the surface chemistry and cellular response of anodized titanium, Apl. Surf. Sci. 349 (2015) 911-915.

[30] E. Gongadze, D. Kabaso, S. Bauer, T. Slivnik, P. Schmuki, U. van Rienen, A. Iglič, Adhesion of osteoblasts to a nanorough titanium implant surface, Int. J. Nanomedicine. 6 (2011) 1801–1816.

[31] M.P. Chávez-Díaz, M.L. Escudero-Rincón, E.M. Arce-Estrada, R. Cabrera-Sierra, Effect of the heat-treated Ti6Al4V alloy on the fibroblastic cell response, Materials. 11 (2018) 1-17.

[32] B.H. Lee, Y.D. Kim, J.H. Shin, K.H. Lee, Surface modification by alkali and heat treatments in titanium alloys, J. Biomed. Mater. Res. 61(3) (2002) 466-473.

[33] Y. Su, S. Komasa, T. Sekino, H. Nishizaki, J. Ozaki, Nanostructured Ti6Al4V alloy fabricated using modified alkali – heat treatment: Characterization and cell adhesion, Mater. Sci. Eng. C Mater. Biol. Appl. 59 (2016) 617-623.

[34] S. Kobayashi, T. Inoue, K. Nakai, Effect of heat treatment on cohesion of films on alkali-treated titanium, Mater. Trans. 46(2) (2005) 207-210.

ACCEPTED MANUSCRIPT

Highlights

- CP and MgCP coatings are deposited on Ti6Al4V substrate by needleless electrospinning
- the conditions of electrospinning process is optimized
- calcination temperature significantly affects the samples morphology
- good adhesion and proliferation activity of cells is shown for 600°C calcined samples

ACCEPTED MANUSCRIPT